Journal of Radiotherapy in Practice

cambridge.org/jrp

Developing a Monte Carlo model for MEVION S250i with HYPERSCAN and Adaptive Aperture™ pencil beam scanning proton therapy system

Bing-Hao Chiang, Austin Bunker, Hosang Jin, Salahuddin Ahmad and Yong Chen

Department of Radiation Oncology, University of Oklahoma Health Sciences Center, Oklahoma City, OK, USA

Original Article

Cite this article: Chiang B-H, Bunker A, Jin H, Ahmad S, and Chen Y. (2021) Developing a Monte Carlo model for MEVION S250i with HYPERSCAN and Adaptive Aperture™ pencil beam scanning proton therapy system. *Journal of Radiotherapy in Practice* **20**: 279–286. doi: 10.1017/S1460396920000266

Received: 4 March 2020
Revised: 1 April 2020
Accepted: 2 April 2020
First published online: 15 May 2020

Key words:
HYPERSCAN; Mevion; Monte Carlo; proton; TOPAS

Author for correspondence:
Dr Yong Chen, 800 NE 13th Street, Department of Radiation Oncology, OKCC LL100, Oklahoma City, OK 73104, USA.
E-mail: yong-chen@ouhsc.edu

Abstract

Aim: As the number of proton therapy facilities has steadily increased, the need for the tool to provide precise dose simulation for complicated clinical and research scenarios also increase. In this study, the treatment head of Mevion HYPERSCAN pencil beam scanning (PBS) proton therapy system including energy modulation system (EMS) and Adaptive Aperture™ (AA) was modelled using TOPAS (TOolkit for PArticle Simulation) Monte Carlo (MC) code and was validated during commissioning process.

Materials and methods: The proton beam characteristics including integral depth doses (IDDs) of pristine Bragg peak and in-air beam spot sizes were simulated and compared with measured beam data. The lateral profiles, with and without AA, were also verified against calculation from treatment planning system (TPS).

Results: All beam characteristics for IDDs and in-air spot size agreed well within 1 mm and 10% separately. The full width at half maximum and penumbra of lateral dose profile also agree well within 2 mm.

Finding: The TOPAS MC simulation of the MEVION HYPERSCAN PBS proton therapy system has been modelled and validated; it could be a viable tool for research and verification of the proton treatment in the future.

Introduction

The number of proton therapy facilities has steadily increased during recent years. Proton therapy, with the characteristic Bragg peak, allows to deliver large doses at Bragg peak region and almost no doses after Bragg peak and has the ability to reduce normal tissue doses while maintaining adequate dose coverage to tumour.[1] The use of protons was found to reduce the mean dose to the organs-at-risks compared to that with the conventional photon therapy for patients suffered from head and neck, paediatric and prostate cancer.[2–5] To ensure patient dose estimation, an accurate dose calculation plays a crucial role in proton therapy. The two main methods of proton dose calculation used in the clinic include analytical algorithms and Monte Carlo (MC) simulations. Analytical algorithms such as pencil beam algorithms were widely applied into treatment planning system (TPS) in clinic because of fast computational speed.[6] On the other hand, MC calculations such as TOPAS have the ability to accurately calculate dose in heterogeneous mediums.[7,8] MC was also proved to be extremely helpful for quality assurance techniques as well as for commissioning commercial TPSs.[9,10]

The two main proton beam delivery techniques used for proton therapy are passively scattered proton therapy (PSPT) and scanning beam proton therapy (SBPT). For PSPT, such as double scattering and single scattering, the lateral and longitudinal spreading of dose deposits are achieved using scattering and range-shifting materials. While SBPT, such as uniform scanning and pencil beam scanning (PBS), involves directly moving a charged particle beam while depositing the dose throughout the target volume. The MEVION S250i with HYPERSCAN and Adaptive Aperture™ (AA) is a single room compact PBS proton therapy system, recently installed and commissioned in our institution, utilises gantry mounted superconducting synchrocyclotron which delivers a pulsed beam with a nominal energy of 230 MeV and allows for 185° rotation having the ability to deliver Intensity Modulated Proton Therapy (IMPT) treatments.

The main objective of the present study has been to provide an overview of the design and commissioning of the first MC model of MEVION S250i with HYPERSCAN and AA for future research, clinical commissioning of such a system and verification of proton treatment.

Materials and Methods

Mevion S250i overview

The MEVION S250i with HYPERSCAN and AA PBS proton therapy system (Mevion Medical Systems Inc., Littleton, MA, USA) is a single room PBS system utilising gantry mounted

CAMBRIDGE UNIVERSITY PRESS

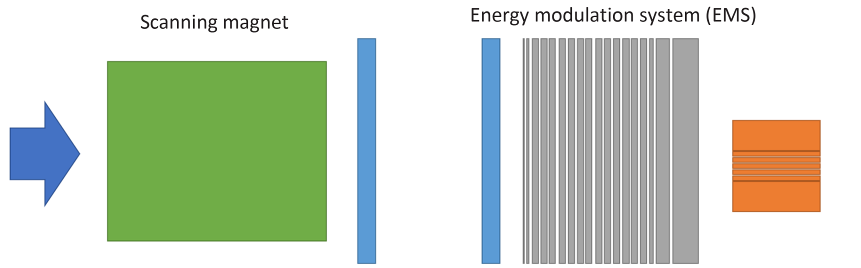

Figure 1. Diagram of the nozzle of Mevion S250i HYPERSCAN system.

superconducting synchrocyclotron. The single room design of this system provides a lower cost option for implementing proton therapy and eliminating the need for a complex beam transport system.[11] The MEVION S250i with HYPERSCAN delivers a pulsed beam with a nominal energy of 230 MeV and utilises 18 Lexan plates, an energy modulation system (EMS), for energy layer switching and proton multi-leaf collimator, the AA, for trimming the edges of the beam at every layer of delivery.

Monte Carlo simulation

The nozzle of Mevion S250i system, including EMS and AA, was modelled using TOPAS (TOolkit for PArticle Simulation) version 3.1.2. TOPAS is a Geant4 simulation extension toolkit which can model X-ray and particle therapy treatment head with user-friendly TOPAS parameter control system. It has been shown to be a useful experimentally validated model for simulating beam data from PBS system.[12] The default physics list containing the Geant4 modules, including "g4em-standard_opt4", "g4h-phys_QGSP_BIC_HP", "g4decay", "g4ion-binary-cascade", "g4h-elastic_HP" and "g4stopping", was used in the simulations without modification. TOPAS has the build-in capability of custom geometry component extension, which allows users to write their own geometry component class with basic concept of C++ and Geant4 geometry. The nozzle of Mevion S250i HYPERSCAN system consists of scanning magnet, two sets of beam profile monitors, EMS and AA (see Figure 1). Each nozzle element was modelled with sub-millimeter accuracy following the detailed information provided by Mevion. Both scanning magnet and two sets of beam profile monitors were modelled using TOPAS build-in geometry. Scanning magnet was modelled by applying TOPAS build-in electromagnetic fields to a cuboid geometry component, and two sets of beam profile monitors were modelled using TOPAS build-in multi wire chamber geometry (TsMultiWoreChamber). On the other hand, the EMS and AA were modelled using in-house geometry component class as described in detail below.

Modeling the EMS

The EMS, which consists of 18 Lexan plates that can move in or out of beam line, has the ability to modulate beam energy and accomplishes range adjustment using 157 unique Lexan plate combinations. The plate arrangement is designed to deliver single shot of protons with range between 0 and 32·2 g/cm^2 with 0·2 g/cm^2 steps. All 18 Lexan plates were modelled using in-house geometry component class extension in TOPAS. The in-house geometry for EMS is designed to accommodate various specifications of 18 Lexan plates, and the user can define the position and dimension of each Lexan plate, such as thickness and material. The component of each Lexan plate was defined using predefined material in TOPAS, and the density of each Lexan plate was then fine-tuned to match with the corresponding range from measurement during commissioning.

Figure 2. IDDs measurement with IBA Blue phantom setup.

Modeling the AA

The AA, which consists of seven pairs of nickel collimator with dynamic positioning that mimics patient-specific aperture, was used to improve the lateral penumbra especially at lower energy beam. The AA has trimming capabilities not offered by typical patient-specific apertures. For example, it has the ability to use distinct apertures for each energy layer within a field and the ability to trim with geometries not achievable with machined static apertures. All seven pairs of nickel collimator were modelled using in-house geometry component class extension in TOPAS. The AA of Mevion HYPERSCAN system was strictly designed that no spot will go beyond the tip of each AA leaf, which will minimise the effect of tongue and groove effect for dosimetry study purpose. Therefore, the in-house geometry for adaptive aperture using

https://doi.org/10.1017/S1460396920000266 Published online by Cambridge University Press

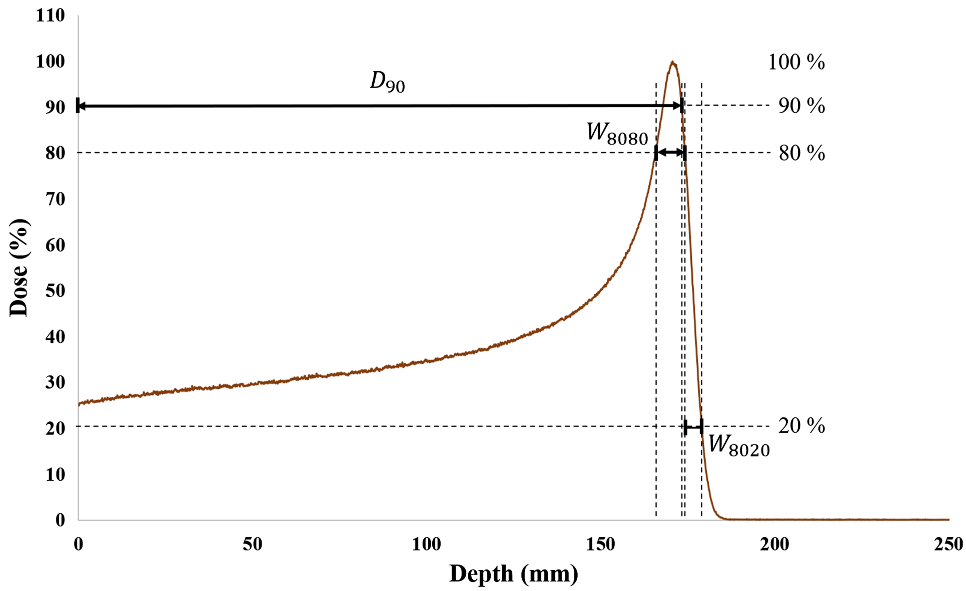

Figure 3. Beam characteristics of pristine Bragg peak including the distal range of 90% dose (D90), width of 80% dose (W8080) and 80% to 20% dose distal fall off (W8020) for benchmarking beam model.

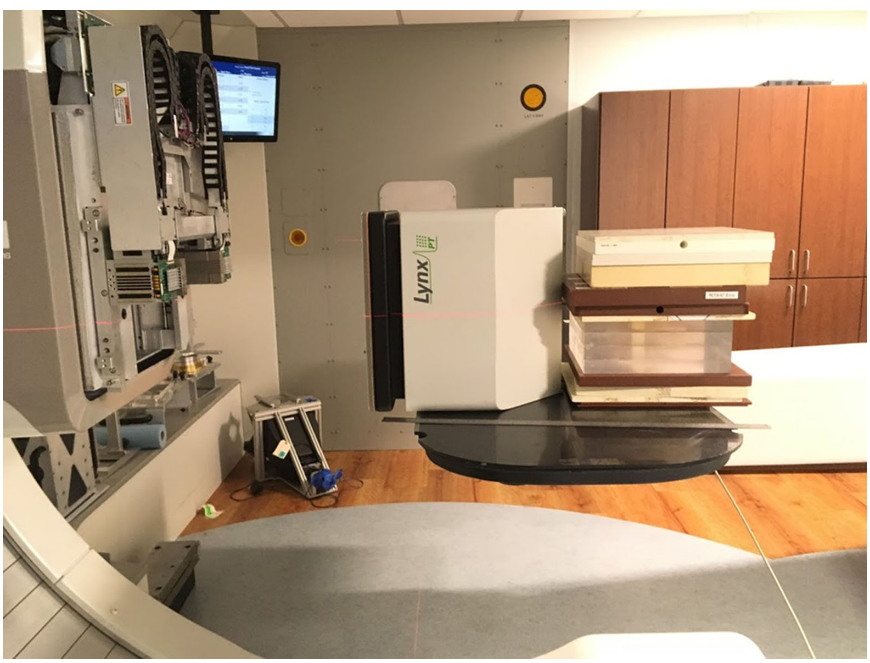

Figure 4. In-air spot size setup showing a 2D scintillator detector, Lynx (IBA Dosimetry).

simplified collimator, which is nondivergent and not considering tongue and groove of collimator, and users can define various dimensions and dynamic positions that mimic patient-specific static aperture.

Pristine Bragg peak validation

The IBA blue phantom as shown in Figure 2 was used for the integral depth dose (IDD) measurements of pristine Bragg peaks. The nominal source to isocentre distance (SID) was 185·0 cm, and water surface level was set at 15·0 cm above the isocentre. A large cylindrical chamber with 12 cm diameter active area (Stingray chamber, IBA Dosimetry) was used for measuring IDDs of the pristine Bragg peaks. Fourteen IDDs with different combinations of 18 Lexan plates for different nominal energies were measured during commissioning for validating calculated IDDs from RayStation TPS. For all 14 IDDs, corresponding combinations of Lexan plates for different nominal energies were simulated in TOPAS. For each simulation, 10^6 protons were run in a $40 \times 40 \times 40$ cm^3 water phantom. The nominal SID and water surface were set at 185·0 cm and 15·0 cm above the isocentre. The geometry of the cylindrical scoring volume was set to match the same diameter as the Bragg peak chamber and a thickness of 0·5 mm.

Figure 3 shows beam characteristics of pristine Bragg peak used for benchmarking beam model. The mean energy of the pristine Bragg peak was evaluated by proton range, which is historically defined by the D90 (90% dose in the distal falloff) of a

https://doi.org/10.1017/S1460396920000266 Published online by Cambridge University Press

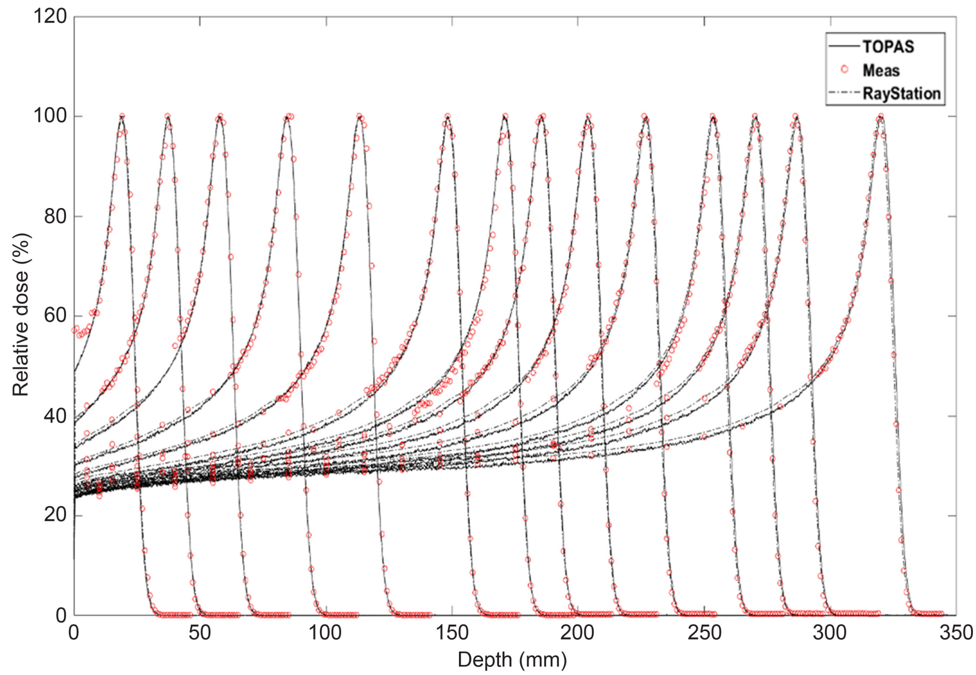

Figure 5. IDDs curve comparison between TOPAS MC data (solid line), measured data (circle) and RayStation TPS data (dash-dot line) for different energies.

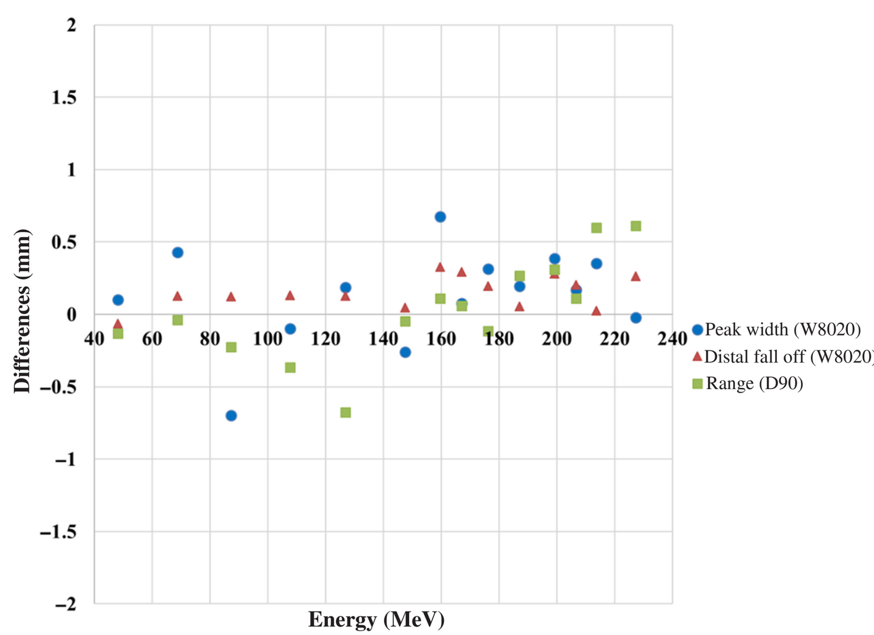

Figure 6. The differences of W_{8080} peak width (blue circle) and W_{8020} distal fall off (red triangle) and D_{90} range (green square) between TOPAS data and measured data at different energies.

pristine Bragg peak. The average energy spread of pristine Bragg peak was evaluated by proton Bragg peak width, which was defined as the width between the proximal position of the 80% and the distal position of the 80% dose levels (W_{8080}). The average dose degradation of the distal falloff region and the width between the distal position of the 80% and 20% dose levels (W_{8020}) were used to compare the difference between simulated pristine Bragg peak and measured Bragg peak.

In order to validate the accuracy of TOPAS simulation, beam characteristics of pristine Bragg peak including the distal range of 90% dose (D90), width of 80% dose (W_{8080}) and 80% to 20% dose distal fall off (W_{8020}) for all IDD curves were calculated and the differences were compared between measurement and simulation.

In-air spot size validation

To ensure that the beam propagation process was simulated correctly, in-air spot size of different energies at different positions was measured and compared with simulation. A 2D dosimetry system (Lynx, IBA Dosimetry), as shown in Figure 4, consisting of a scintillator screen coupled with a CCD camera, with 0·5 mm resolution and 30x30 cm^2 active area, was used for in-air spot size measurements. The in-air spot sizes of 33·04 MeV, 100·25 MeV, 147·36 MeV, 190·82 MeV and 227·15 MeV were measured at ±10 cm, ±20 cm and isocentre. For TOPAS, the in-air spot sizes of corresponding energies and positions were simulated. For each simulation, 10^8 protons were run.

https://doi.org/10.1017/S1460396920000266 Published online by Cambridge University Press

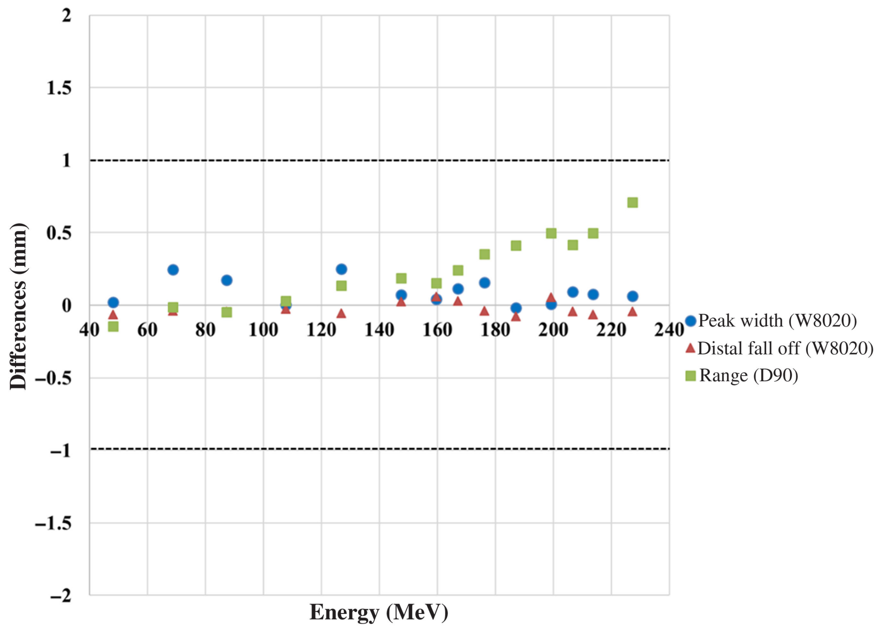

Figure 7. The differences of W_{8080} peak width (blue circle) and W_{8020} distal fall off (red triangle) and D_{90} range (green square) between TOPAS data and RayStation data at different energies.

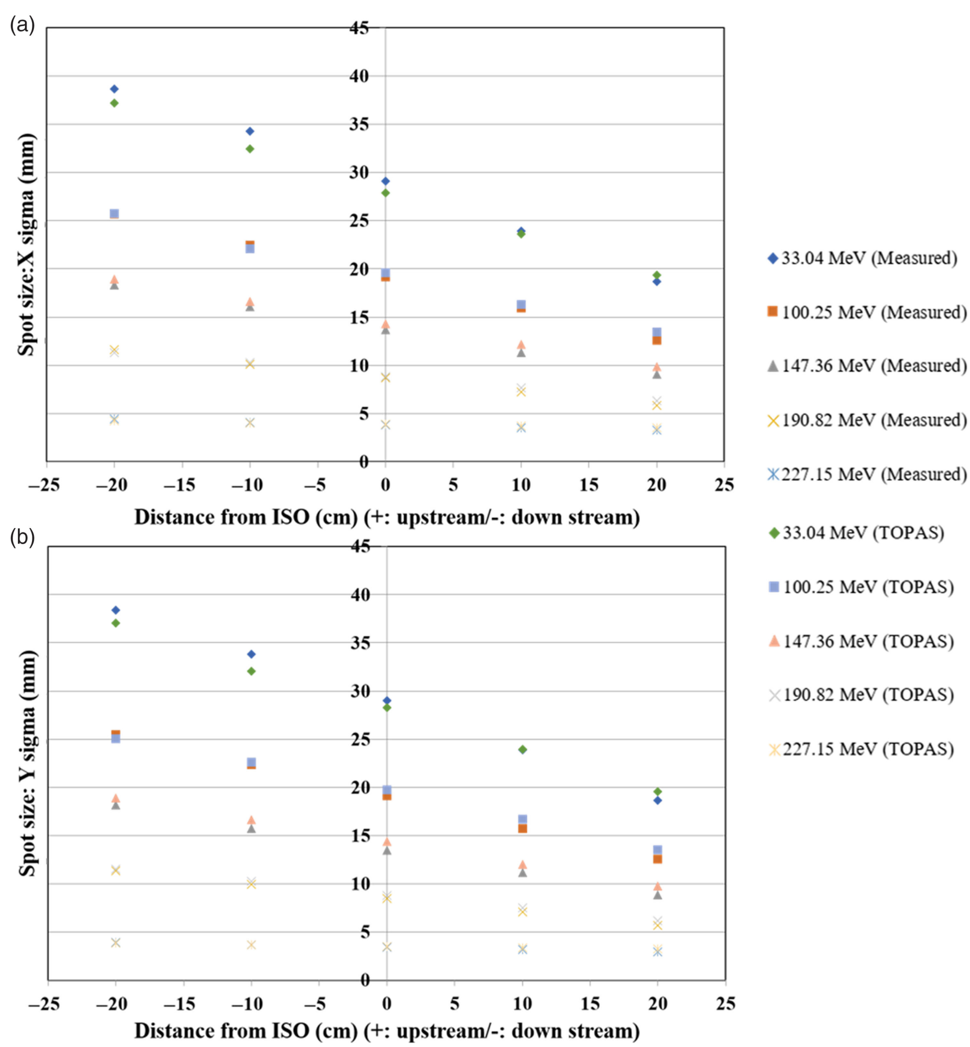

Figure 8. Spot sizes comparison for different energies at different positions. (a) Comparison of spot size at x direction (σ_x) from both simulation and measurement. (b) Comparison of spot size at y direction (σ_y) from both simulation and measurement.

https://doi.org/10.1017/S1460396920000266 Published online by Cambridge University Press

Table 1. Comparison of field size (FWHM) and 20–80% penumbra of lateral dose profile at 10 cm depth with and without AA between calculation (RayStation) and MC simulation (TOPAS) data for 5 × 5 cm^2 230 MeV proton plane beam

	With AA			No AA		
Energy = 230 MeV	RayStation	TOPAS	Difference	Ray Station	TOPAS	Difference
Field size (X) (mm)	50·32	49·59	0·73	52·62	52·80	−0·18
Penumbra Lt (X) (mm)	4·53	4·15	0·38	7·01	7·15	−0·14
Penumbra Rt (X) (mm)	4·53	4·28	0·25	7·11	7·13	−0·02
Field size (Y) (mm)	49·62	48·40	1·22	52·63	52·68	−0·05
Penumbra Lt (Y) (mm)	4·62	3·52	1·10	7·18	7·82	−0·64
Penumbra Rt (T) (mm)	3·72	3·73	−0·01	6·97	7·82	−0·84

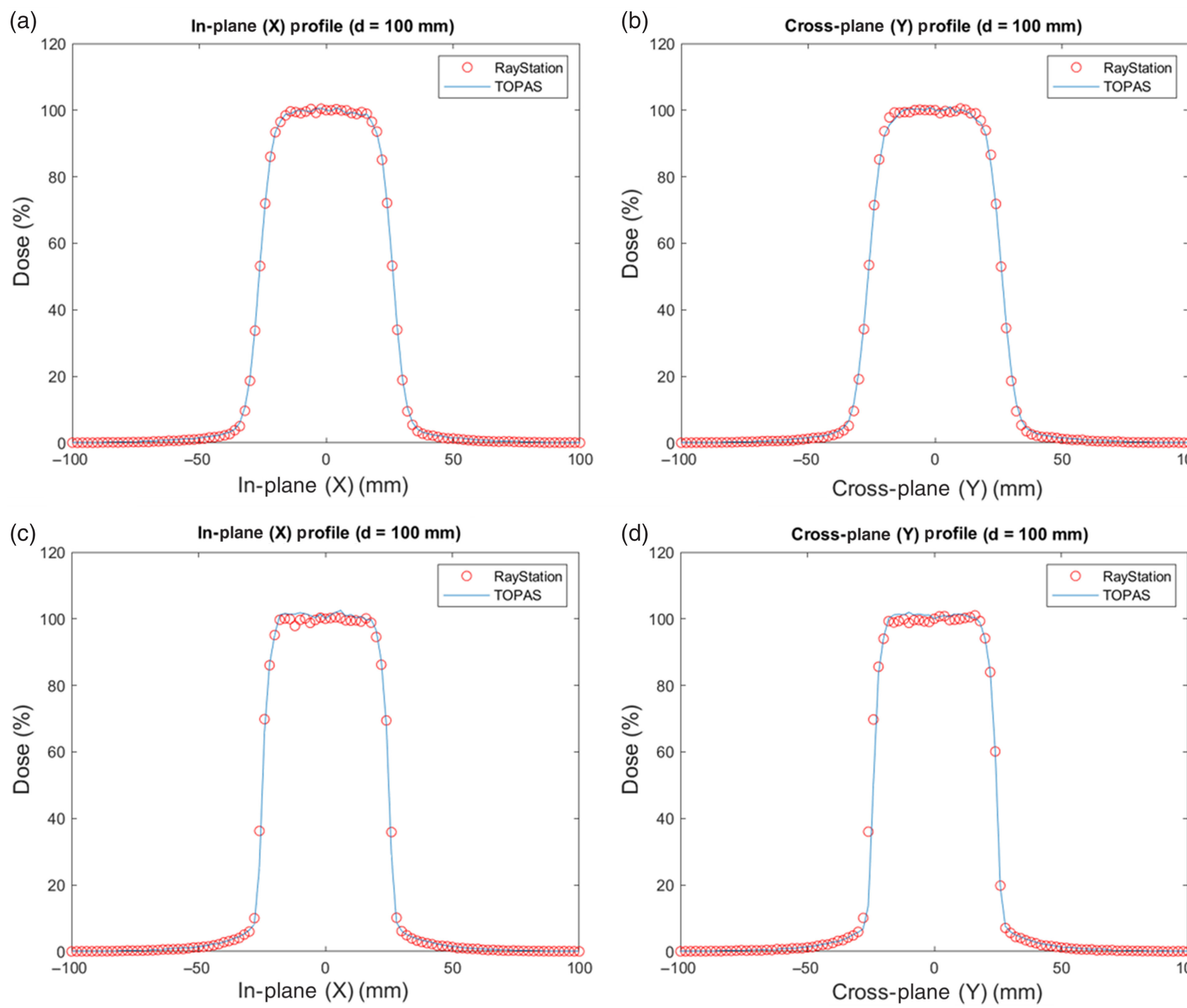

Figure 9. Normalised lateral profiles of 230 MeV at 10 cm depth in the water from the RayStation treatment planning system (red) and simulation (blue) without AA in (a) in-plane direction and (b) cross-plane direction and with AA in (c) in-plane direction and (d) cross-plane direction.

For beam spot size validation, in-air spot sizes in both x and y directions were calculated and the differences between measurements and simulations were compared. For beam spot size validation, the spot sizes in both x and y directions for all different positions between measured and simulated were also compared.

Lateral dose profile validation

To validate the lateral dose profile, a plan with a 5 × 5 cm^2 uniform dose distribution centred at 10 cm depth in a 30 × 30 × 30 cm^3 water phantom was made with RayStation TPS. An in-house Matlab-based tool was used to convert pulse by pulse physics

https://doi.org/10.1017/S1460396920000266 Published online by Cambridge University Press

Table 2. Comparison of field size (FWHM) and 20–80% penumbra of lateral dose profile at 10 cm depth with and without AA between calculation (RayStation) and MC simulation (TOPAS) data for 5 × 5 cm² 160 MeV proton plane beam

	With AA			No AA		
Energy = 160 MeV	RayStation	TOPAS	Difference	RayStation	TOPAS	Difference
Field size (X) (mm)	50·17	49·80	0·37	52·99	53·51	−0·52
Penumbra Lt (X) (mm)	11·49	11·45	0·04	16·57	18·07	−1·50
Penumbra Rt (X) (mm)	11·46	11·50	−0·04	16·73	18·26	−1·53
Field size (X) (mm)	49·68	48·74	0·94	53·25	53·53	−0·27
Penumbra Lt (X) (mm)	11·48	10·78	0·70	16·62	18·33	−1·71
Penumbra Rt (X) (mm)	10·94	11·08	−0·14	16·83	17·98	−1·15

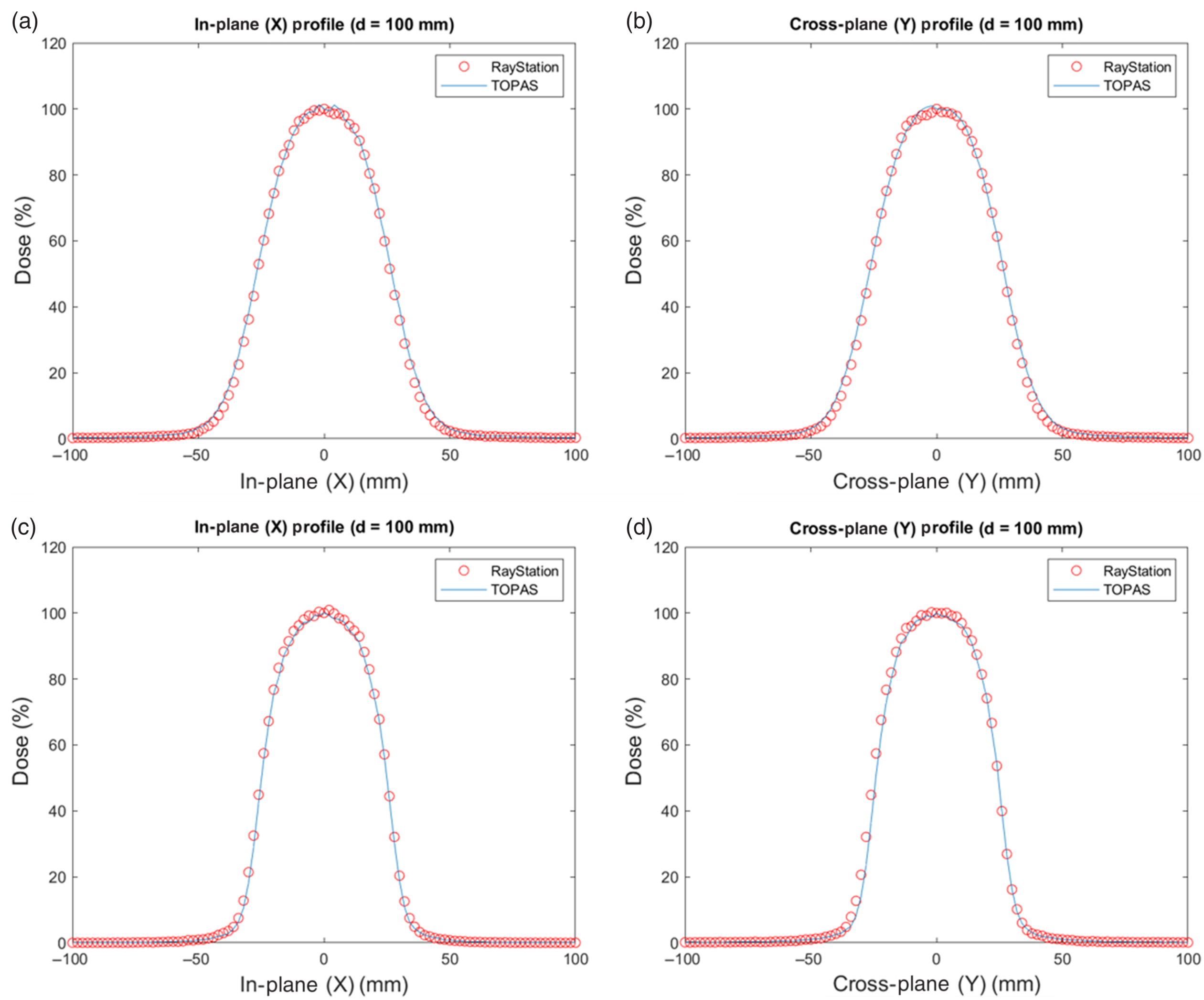

Figure 10. Normalised lateral profiles of 160 MeV at 10 cm depth in the water from the RayStation treatment planning system (red) and simulation (blue) without AA in (a) in-plane direction (b) cross-plane direction and with AA in (c) in-plane direction (d) cross-plane direction.

and geometry information (beam energy, charge per pulse, spot positions, energy selectors combination and AA positions) from the delivered machine log file to TOPAS time feature file for creating simulation of validation plan, which was consisted of 100 million protons for achieving both accuracy and efficiency of the simulation. To validate the AA modelling, the 2D profiles, with and without AA, in both in-plane and cross-plane directions were compared between calculations and simulations. The relative dose comparison was normalised to the iso-centre. For each 2D profile, the full width at half maximum (FWHM) and penumbra were compared. The penumbrae were calculated as the distance between the 80% and 20% dose levels.

https://doi.org/10.1017/S1460396920000266 Published online by Cambridge University Press

Results and Discussion

Pristine Bragg peak comparison

To compare with corresponding measured IDDs of pristine Bragg peak, the simulated data for each energy were normalised to 100% at maximum dose. Figure 5 compares IDDs between TOPAS MC-simulated data, measured data during commissioning and RayStation TPS data for all 14 energies. As shown in Figure 6, all beam characteristics including peak width, distal fall-off and range of pristine Bragg peak of 14 energies exhibited good agreement within 1 mm between simulated data and measured data. The beam characteristics of peak width, distal fall-off and range of pristine Bragg peak were also compared between simulation data from TOPAS and calculation data from RayStation for 14 energies. As shown in Figure 7, the differences of beam characteristics are also agreed well within 1 mm tolerance.

In-air lateral profile comparison

The spot profiles show Gaussian beam distributions measured in-air for five energies: 33·04, 100·25, 147·36, 190·82 and 227·15 MeV. The comparison between measured and simulated spot sizes in σ_x and σ_y for five different energies at five different positions is shown in Figure 8. The differences of beam spot sizes between measured and simulated data agreed well within 10% tolerance.

Lateral dose profile comparison

The 5×5 cm^2 calculated and simulated lateral dose profiles for 230 MeV and 160 MeV beam in the water, both with and without AA, are shown in Figures 9 and 10. The lateral profile agrees well between calculation and simulation, and the AA shows the ability of sharpening field size and penumbra for both energy and both directions. Table 1 and 2 list the comparison of FWHM and 20–80% penumbra for the lateral dose profile with and without AA at 10 cm depth between calculated and simulated lateral profile for 230 MeV and 160 MeV, respectively. The FWHM and 20–80% penumbra agree well within 2 mm for both energy and direction.

Conclusions

In this study, the beam model of MEVION S250i with HYPERSCAN and AA PBS proton therapy system was modelled and validated. The beam line components including EMS and AA were modelled in detail and showed promising results of agreements with both pristine Bragg peak and in-air profile measurement taken during commissioning. The validation of the lateral dose profile in water between simulation and treatment plan also showed well in agreement. The future studies including patient-specific dose calculation/validation with the delivered machine log information will be conducted. The TOPAS MC simulation of the MEVION S250i with HYPERSCAN and AA PBS proton therapy system could thus serve in future a viable tool for research and verification of the proton treatment.

Acknowledgements. The authors would like to thank Mr. Daniel Green and Nathan Gilley from MEVION service engineering team for their assistance during beam data collection.

References

1. Wilson R R. Radiological use of fast protons. Radiology 1946; 47: 487–491.
2. Boehling N S, Grosshans D R, Bluett J B et al. Dosimetric comparison of three-dimensional conformal proton radiotherapy, intensity-modulated proton therapy, and intensity-modulated radiotherapy for treatment of pediatric craniopharyngiomas. Int J Radiat Oncol Biol Phys 2012; 82: 643–652.
3. Mock U, Georg D, Bogner J, Auberger T, Pötter R. Treatment planning comparison of conventional, 3D conformal, and intensity-modulated photon (IMRT) and proton therapy for paranasal sinus carcinoma. Int J Radiat Oncol Biol Phys 2004; 58: 147–154.
4. Vargas C, Fryer A, Mahajan C et al. Dose–volume comparison of proton therapy and intensity-modulated radiotherapy for prostate cancer. Int J Radiat Oncol Biol Phys 2008; 70: 744–751.
5. Yock T, Schneider R, Friedmann A, Adams J, Fullerton B, Tarbell N. Proton radiotherapy for orbital rhabdomyosarcoma: clinical outcome and a dosimetric comparison with photons. Int J Radiat Oncol Biol Phys 2005; 63: 1161–1168.
6. Hong L, Goitein M, Bucciolini M et al. A pencil beam algorithm for proton dose calculations. Phys Med Biol 1996; 41: 1305.
7. Perl J, Shin J, Schümann J, Faddegon B, Paganetti H. TOPAS: an innovative proton Monte Carlo platform for research and clinical applications. Med Phys 2012; 39: 6818–6837.
8. Testa M, Schümann J, Lu H M et al. Experimental validation of the TOPAS Monte Carlo system for passive scattering proton therapy. Med Phys 2013; 40: 121719.
9. Chung K, Kim J, Kim D-H, Ahn S, Han Y. The proton therapy nozzles at Samsung Medical Center: a Monte Carlo simulation study using TOPAS. J Korean Phys Soc 2015; 67: 170–174.
10. Prusator M, Ahmad S, Chen Y. TOPAS simulation of the Mevion S250 compact proton therapy unit. J Appl Clin Med Phys 2017; 18: 88–95.
11. Smith A R. Vision: proton therapy. Med Phys 2009; 36: 556–568.
12. Lin L, Kang M, Solberg T D, Ainsley C G, McDonough J E. Experimentally validated pencil beam scanning source model in TOPAS. Phys Med Biol 2014; 59: 6859–6873.